Global Journal of Engineering and Technology Advances
eISSN: 2582-5003
Cross Ref DOI: 10.30574/gjeta
Journal homepage: https://gjeta.com/

(RESEARCH ARTICLE)

Check for updates

Generative design and structural optimization of a hexacopter frame for agricultural UAV spraying

Yamral Kassanew Akele [1,*] and Belaynesh Kassanew Akele [2]

[1] *Graduate Institute of Intelligent Manufacturing Technology, National Taiwan University of Science and Technology, No. 43, Keelung Rd, Sec.4, Da'an Dist., Taipei 10607, Taiwan.*
[2] *Graduate Institute of Digital Learning and Education, National Taiwan University of Science and Technology, No. 43, Keelung Rd, Sec.4, Da'an Dist., Taipei 10607, Taiwan.*

Global Journal of Engineering and Technology Advances, 2025, 24(01), 067-086

Publication history: Received on 02 June 2025; revised on 08 July 2025; accepted on 11 July 2025

Article DOI: https://doi.org/10.30574/gjeta.2025.24.1.0217

Abstract

This study presents a generative design-based optimization of a hexacopter drone frame intended for agricultural spraying applications. Utilizing artificial intelligence-driven algorithms within Autodesk Fusion 360, the research explores multiple frame configurations based on structural constraints and performance objectives. Finite Element Method (FEM) simulations, conducted through both ANSYS and Fusion 360, modeled dynamic operational scenarios such as landing impacts and aerial collisions. These simulations enabled the identification of overstressed regions, leading to iterative material removal and geometric refinement. The finalized frame design achieved a mass of 2.784 kg, translating to a 7.2% to 38.1% reduction compared to traditional 10-liter agricultural drone frames, while maintaining a high safety factor range of 9.60 to 15 and a maximum displacement of just 1.288 mm. Furthermore, flight performance analysis indicated a linear reduction in throttle requirement from 80% to 32.6% as tank weight decreased from 16.88 kg to 6.88 kg, thereby extending flight duration from 6 to 14.6 minutes. These results demonstrate the effectiveness of generative design for developing structurally efficient and operationally robust UAV frames. Future research will explore foldable design strategies to further enhance portability and field adaptability.

Keywords: Agricultural drone; Finite Element Method; Flight performance analysis; Generative design; Structural optimization; UAV frame design

1. Introduction

In recent years, the agricultural sector has increasingly embraced drone technology to address the pressing need for precision, efficiency, and cost-effectiveness in farming operations. Drones, also known as Unmanned Aerial Vehicles (UAVs), have been widely recognized for their ability to perform diverse agricultural tasks such as crop monitoring, pesticide spraying, and field mapping. These systems offer improved data accuracy, reduced operational costs, and enhanced crop productivity, positioning them as key enablers of modern precision agriculture [1] and [2].

Historically, Japan was a pioneer in using drones for agricultural spraying applications as early as the 1980s, leading to a broader global interest in integrating UAVs into agricultural workflows [3]. The economic impact of drone usage in agriculture is significant. Studies have shown that drone integration can lead to annual cost savings of up to $1.3 billion for wheat and soybean farmers in the U.S., with yield increases between 2.5% and 3.3%, and ROI reaching as high as 146% in some regions [4] and [5].

* Corresponding author: Yamral Kassanew Akele

Despite these benefits, commercially available drone frames often fall short in terms of weight efficiency, structural resilience, and adaptability to specific agricultural tasks. Off-the-shelf designs tend to lack customization, resulting in excess weight that diminishes flight endurance and payload capacity. Moreover, they are rarely optimized to withstand high-frequency vibrations from spinning rotors or absorb impact forces from landings, both of which are critical for maintaining UAV reliability in rugged farming environments [6].

Conventional manufacturing techniques impose geometric constraints on drone frame design, which often limits performance optimization. These techniques can result in over-engineered parts with redundant materials, increasing overall mass and decreasing aerodynamic efficiency [7]. Addressing this challenge requires design methodologies that not only meet structural demands but also facilitate weight minimization without compromising mechanical robustness. Lightweight frames reduce energy consumption, prolong flight duration, and improve payload capacity, all of which are critical parameters for efficient agricultural UAV operation [8].

Generative design a computational approach that iteratively explores optimized geometries within specified constraints has emerged as a powerful tool for producing lightweight yet structurally robust drone components. This method, particularly when combined with additive manufacturing (3D printing), enables engineers to create drone frames that are tailored to specific use cases, balancing performance and manufacturability [9] , [10]and [11]. Additive manufacturing further enhances the design process by allowing the fabrication of complex topologies that would be difficult or impossible to produce using conventional manufacturing methods.

Structural performance analysis is equally vital in ensuring that UAV frames endure the mechanical stresses encountered during operation. Finite Element Method (FEM)-based simulation tools such as ANSYS and Fusion 360 enable accurate evaluation of stress distributions, modal behavior, deformation, and fatigue life under various loading conditions. These simulations are instrumental in identifying overstressed regions and guiding material distribution strategies that ensure safety and reliability [12].

The integration of drones into agricultural operations has prompted significant research on structural optimization and UAV design. Studies have investigated material selection, geometric configurations, and topology optimization strategies to improve drone performance. analyzed various lightweight structural materials for UAV frames, noting that carbon-fiber-reinforced composites offer an ideal balance of strength and weight for aerial applications. Similarly, Sone and Kaneko (2021) explored the impact of vibration-resilient frame designs on drone stability during pesticide spraying.

Generative design has been increasingly applied in drone and aerospace applications for producing lightweight components with tailored mechanical properties. Applied generative design methods in Autodesk Fusion 360 to minimize mass in drone arm structures while maintaining deflection constraints [13]. Their results revealed up to 40% mass reduction compared to traditional CAD designs, with improved stiffness-to-weight ratios. Likewise, demonstrated that generative designs for UAV brackets outperformed manually designed counterparts in modal analysis, achieving higher natural frequencies and reduced resonance risks [14].

In agricultural contexts, frame design must accommodate payload variability, environmental exposure, and terrain-induced landing shocks. reviewed FEM analyses showing that stress concentrates around rotor hubs and payload mounts during rough landings supporting the need for targeted reinforcement zones as reviewed by [15]. Similarly, FEM simulations on a 30 kg hexacopter and proposed reinforcement strategies to resiliently absorb impact forces during field landings, ensuring critical load-bearing regions maintain structural integrity as conducted by [16].

3D printing and additive manufacturing technologies have also facilitated the realization of generatively designed UAV structures. A hexacopter prototype constructed using fused deposition modeling (FDM) with PLA and fiber-reinforced PA12 successfully met structural requirements [8], while reducing total weight significantly compared to conventional aluminum frames [17].

Despite these advancements, limited studies have holistically integrated generative design with structural simulation and additive manufacturing in agricultural drone development. Most prior works focus on either material optimization, modal analysis, or topology refinement in isolation. This study addresses that gap by combining generative design with FEM analysis and additive fabrication in the development of a structurally efficient, application-specific hexacopter frame.

This study proposes the use of generative design techniques to develop a hexacopter drone frame specifically tailored for agricultural applications. The frame will be fabricated using 3D printing to leverage the design freedom of additive

manufacturing. Particular attention is given to optimizing structural integrity under two key mechanical conditions: fatigue loading induced by continuous rotor vibration, and sudden impact from landings or collisions. The study aims to demonstrate that combining generative design with additive manufacturing can produce a structurally efficient, lightweight, and application-specific drone frame capable of withstanding operational demands in precision agriculture.

2. Methodology

This study employed a structured methodology that integrates generative design principles, simulation-based structural analysis, and design validation, specifically tailored for agricultural drone applications. The primary objective was to develop an optimized hexacopter frame capable of withstanding field-induced dynamic and impact loads while minimizing structural weight through advanced design strategies. The overall methodological framework illustrated in Figure 1 systematically connects UAV requirements, design exploration, simulation, and performance evaluation. Each stage was iteratively refined based on simulation feedback and real-world constraints. The use of Autodesk Fusion 360 enabled seamless transition from conceptual modeling to performance-based optimization. Together, these steps ensured a balance between manufacturability, mechanical robustness, and mission-specific efficiency. This process is organized into five core stages, as described below.

- Product Specification and Requirements Definition: A literature review informed the selection of structural materials, geometry, and design constraints based on agricultural UAV needs—such as payload capacity, tank size, and flight endurance. These parameters defined the design envelope for additive manufacturing.
- Generative Design and Simulation: Autodesk Fusion 360 was used to apply generative design techniques using PLA and ABS. PLA was preferred for its higher stiffness. The tool generated multiple lightweight configurations, and the most structurally efficient design was selected for further analysis.
- Fatigue Analysis: Cyclic motor vibrations were simulated using ANSYS to evaluate fatigue life through S-N curves and the Goodman criterion. Stress concentrations were primarily observed at the motor mount junctions, yet the results confirmed long-term operational reliability. The analysis showed that the material endurance limits for ABS were not surpassed, ensuring resistance to crack initiation and propagation under fluctuating loads. These results validate the drone frame's durability under repeated flight cycles and support its suitability for sustained agricultural missions.
- Impact Resistance Analysis: Transient simulations modeled sudden landing and collision scenarios. Von Mises stress and deformation results demonstrated that the frame could withstand impact without structural failure.
- Validation and Manufacturing Consideration: The final design was validated for both performance and printability using FDM. Slicing simulations confirmed feasible fabrication, and the PLA prototype was deemed suitable for production.

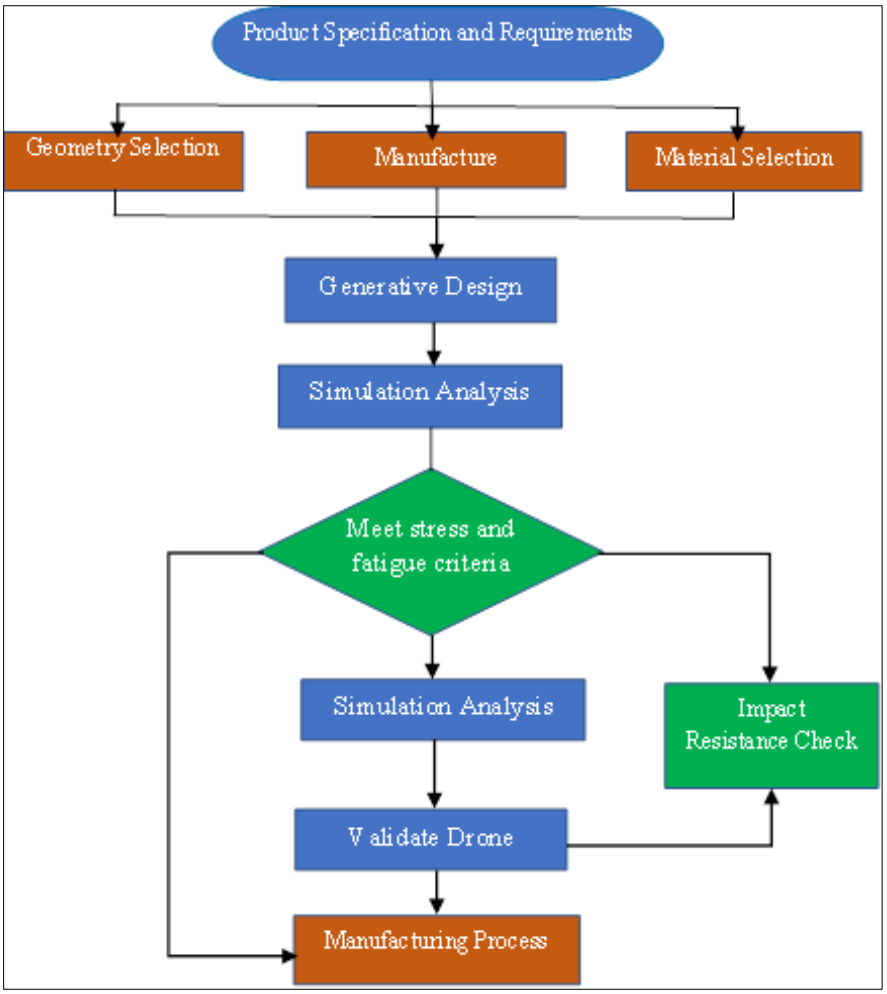

Figure 1 Methodology flow diagram for drone frame development and optimization

3. Concept Design

3.1. Conceptual Design and Geometry Selection

The agricultural drone frame was conceptually designed to balance lightweight structure, mechanical strength, and functional performance. Generative design software explored structural variations such as arm thickness, cross-sections, and internal lattice geometries to reduce material use without sacrificing integrity [10]. 3D modeling and Finite Element Analysis (FEA) were used in tandem to assess the mechanical behavior of each candidate design under simulated flight conditions. This iterative process ensured alignment between structural performance and manufacturing constraints, producing an efficient and field-ready frame.

Key performance factors fatigue resistance, impact absorption, and weight efficiency guided the configuration. Fatigue simulations modeled cyclic rotor-induced stresses, while impact tests evaluated the frame's ability to handle landing shocks and vibrations. Generative design helped optimize the frame's stiffness-to-weight ratio. From these insights, technical requirements were defined to ensure payload capacity, 3D printability, emergency resilience, durability through repeated use, and manufacturability.

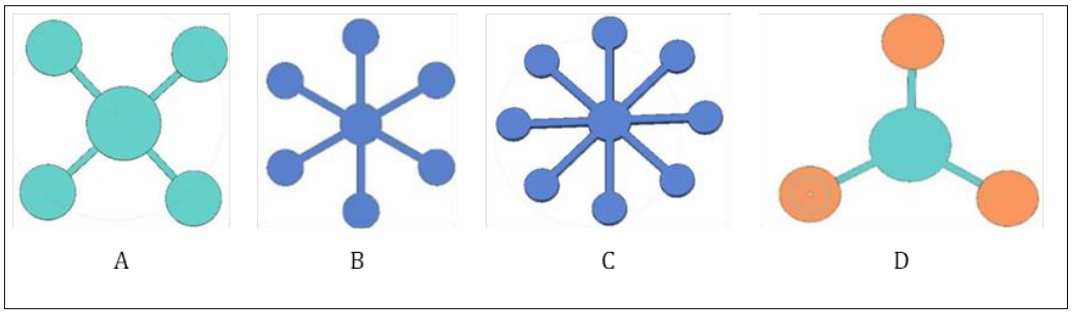

Figure 2 Quadcopter (a), hexacopter (b), Octocopter (c), and tricopter (d)

The drone frame's geometry was critically selected to optimize aerodynamic efficiency, payload support, and system stability. Various configurations quadcopter, hexacopter, octocopter, tricopter, and fixed-wing—were analyzed. Quadcopters (Figure 2a) offer stable control and simplicity, making them highly maneuverable in confined areas [18]. Hexacopters (Figure 2b) enhance thrust and provide fault tolerance due to their six-rotor redundancy ideal for heavier agricultural payloads . Octocopters (Figure 2c) deliver even higher lift capacity and improved redundancy, though at the cost of added weight and complexity [19]. Tricopters (Figure 2d) emphasize maneuverability with fewer rotors but require more complex control tuning and are less stable [20]. Fixed-wing drones enable long endurance flights and efficient area coverage, yet are limited in confined field operations due to requiring forward motion and larger launch space [21].

A weighted decision matrix, based on safety, payload, stability, maneuverability, impact resistance, manufacturability, and cost, was used to evaluate each configuration. As shown in Table 1, the hexacopter scored the highest (3.25), confirming its suitability due to its superior payload capacity, structural redundancy, and ease of manufacturing. Thus, the hexacopter was selected as the optimal platform for the agricultural drone design.

Table 1 Selection of drone frame geometries

Selection characteristic	**Drone frame geometries**										
	Wight	**Quadcopter:**		**Hexacopter**		**Tri copter**		**Octocopter:**		**Fixed-Wing**	
Safety	12 %	2	0.24	3	0.36	1	0.12	3	0.36	4	0.48
Pay load	14%	1	0.14	4	0.56	0	0	3	0.42	4	0.56
Stability and Control	8%	4	0.32	3	0.24	1	0.08	2	0.16	0	0
Manoeuvrability	6%	3	0.18	2	0.12	4	0.24	1	0.06	0	0
Impact	8%	2	0.16	4	0.32	3	0.24	1	0.08	0	0
Manufacturability	9%	4	0.36	3	0.27	2	0.18	1	0.9	0	0
Maintainability	10%	3	0.3	3	0.3	4	0.4	1	0.1	0	0
Complexity	12%	4	0.48	3	0.36	1	0.12	2	0.24	0	0
Cost-effectiveness	11%	3	0.33	3	0.33	4	0.44	1	0.11	0	0
Flight Time	13%	2	0.26	3	0.39	1	0.13	1	0.13	4	0.52

3.2. Manufacturability and Material Selection

Table 2 Manufacturability and Material Selection

Material	**PLA**	**ABS**	**PA**	**PP**	**PS**	**PC**	**TPU**	**ASA**	**PET**	**PE EK**	**PE KK**	**PEi**
Density g/cm^3	1.28	1.08	1.13	0.93	1.05	1.20	1.45	1.08	1.26	1.34	1.28	1.38
Water Absorption %	0.244	0.414	1.710	0.017	0.096	0.186	0.238	0.307	0.16	0.579	0.30	0.22

Tensile Strength, Ultimate	62.4	38.7	70.1	26.6	27.4	66.9	64.5	45.5	41.8	99.5	73.1	131
Tensile Strength, Yield MPa	40.5	45	72	26.7	25.9	61.0	63.6	44.4	47.6	98.0	78.1	11
Modulus of Elasticity GPa	2.27	2.05	1.47	1.32	1.99	2.36	2.58	2.13	2.59	4.0	3.32	7.68
Charpy Impact, Unnotched J/cm^2	2.64	15.4	21.0	3.65	7.70	6.0	12.7	7.8	6.94	10.9	4.87	3.20
Deflection Temp. at 0.46 MPa °C	83	94.6	172	96.8	86.8	129	142	96.3	73.5	200	150	280
Max Service Temp, Air °C	179	89.2	116	122	106	122	141	96.2	67.2	673	257	18

The manufacturability of the hexacopter drone frame was a central consideration during the conceptual and detailed design stages. Additive manufacturing was selected due to its design freedom, material efficiency, and ability to produce complex geometries that traditional subtractive methods cannot achieve. Among various 3D printing methods, Fused Deposition Modeling (FDM) was chosen for its accessibility, affordability, and suitability for prototyping drone structures. FDM enables layered deposition of thermoplastic materials, which is ideal for fabricating large, lightweight airframe structures. However, material compatibility with FDM constraints such as thermal shrinkage, layer adhesion, and build platform limitations was rigorously analyzed to ensure printability and mechanical performance [22]. Table 2 Material properties of candidate materials

A comprehensive material selection process was followed to identify the optimal thermoplastic for drone frame fabrication. The materials evaluated included PLA, ABS, PA, PP, PS, PC, TPU, ASA, PETG, PEEK, PEKK, and PEI. Their mechanical, thermal, and physical properties were compiled and compared in Table 2, which includes data on density, tensile strength, modulus of elasticity, impact resistance, water absorption, and heat deflection temperature. The data were sourced from publicly available engineering material databases and manufacturer datasheets [23].

3.3. General specification for design of agricultural drone frame

To ensure the drone can achieve stable lift and maneuverability, the propulsion system consisting of motors, propellers, battery, and Electronic Speed Controllers (ESCs) must produce sufficient thrust to overcome the drone's total weight. Thrust refers to the upward force generated by the propellers and is expressed in Newtons (N), where 1 N≈0.102 kg. To determine the total required thrust, the following values and formulas were used: the total estimated mass of the drone, which includes the frame, a 10-liter liquid payload, pump, and electronics, is defined as Mass drone. To calculate the thrust needed to keep the drone hovering (i.e., to balance its own weight), the following equation was applied [24]:

$$T_{Hover} = Mass_{drone} \times 9.81\ m/s^2 \quad \text{..... (1)}$$

To ensure the drone can perform take-off and in-flight maneuvers, a thrust-to-weight ratio (TWR) of 1.5 was considered. The total thrust required is given by:

$$T_{Total} = TWR \times T_{Hover} \quad \text{..... (2)}$$

Substituting the relevant values into Eq. (1) – (3), the calculated results were as follows: The required hovering thrust was 165.59 N (Eq. 1), and the total thrust required for stable operation was 248.4 N (Eq. 2).

The drone utilizes a hexacopter frame, meaning it is powered by six motors. To determine the minimum thrust required from each motor, the following formula was applied:

$$T_{motor} = \frac{T_{Total}}{N_{motors}} \quad \text{..... (3)}$$

Substituting the relevant values into Eq. (3), the minimum thrust per motor was found to be 41.4 N.

These calculated thrust values serve as design criteria for selecting suitable motors and propellers in the subsequent component selection stage.

In the drone industry, brushless motors are the preferred choice due to their design, which incorporates a permanent magnet rotor rotating around a stationary armature. Compared to brushed DC motors, brushless motors offer superior efficiency, reduced maintenance, higher torque-to-weight ratio, quieter performance, and extended operational life [25]. For the current hexacopter configuration, the T-Motor 4008 KV230 was selected due to its ability to deliver approximately 4.2 kgf (41.4 N) of thrust at full throttle, satisfying the required lift force per motor. This selection was guided by the need to match the drone's total thrust demand while ensuring compatibility with system parameters [26].

To determine the acceptable performance limits for stable lift, the minimum required thrust per motor was calculated by equally distributing the total thrust across the six motors, using the equation:

$$T_{\text{min each motor}} = \frac{T}{N_{\text{motors}}} \quad \text{..... (4)}$$

Substituting the values into Eq. (4), the total thrust requirement of the drone was based on a fully loaded take-off weight of 25.2 kg, multiplied by the gravitational constant (9.81 m/s^2), resulting in a total lift force of approximately 247.2 N. Dividing this total thrust by six motors, the minimum required thrust per motor was determined to be 41.4 N. This value confirms that each T-Motor 4008KV230, rated at 41.4 N, provides just enough thrust to ensure stable flight under full-load conditions. This ensures adequate lift capacity while maintaining optimal efficiency for agricultural drone operations [27].

3.4. Design of geometry

The geometry of the drone frame critically affects its structural efficiency, particularly its strength-to-weight balance during flight. In vertical or horizontal motion, the UAV encounters lift, drag, thrust, and weight, with horizontal flight introducing a thrust vector with both vertical and horizontal components. Each arm of the hexacopter acts as a cantilever beam, fixed at the center and bearing the motor and propeller at its tip, thus experiencing downward forces from both gravity and aerodynamic loading.

The force along each arm can be modeled as:

$$T = L = \frac{W_{\text{total}}}{N} \quad \text{..... (5)}$$

where Wtotal is the total drone weight and NNN is the number of arms. The beam's deflection under load depends on the material's Young's Modulus (E), highlighting the importance of material selection in frame design [28].

3.5. Design of Length Drone Arm

The drone arm is modeled as a cantilever beam with an I-beam cross-section, which provides high strength-to-weight efficiency due to its structural geometry. This makes the I-beam a preferred choice for lightweight drone applications. For material selection, ABS (Acrylonitrile Butadiene Styrene) is chosen due to its excellent impact resistance, moderate stiffness, and ease of fabrication. The relevant material properties of ABS used in this study are summarized in Table 3.

Table 3 ABS material properties

Property	Symbol	Value	Unit
Yield Strength	σ	≈ 40	MPa
Young's Modulus	E	≈ 2,100	MPa(2.1 GPa)
Density	ρ	≈ 1,040	kg/m^3
Poisson's Ratio	ν	≈ 0.37	--

A cantilever beam is fixed at one end while the other remains free, allowing it to support loads and resist bending and deflection. The assumed I-beam geometry includes a flange width b=0.04m, web height h=0.04m, and web thickness t=0.01m. The moment of inertia I for the I-beam cross-section is calculated using Eq. (6):

$$I = \frac{bh^3 - (b-t)(h-2t)^3}{12} \quad \text{..... (6)}$$

Substituting the dimensions, the moment of inertia is found to be: I = $1.933 * 10^{-7} m^4$

To ensure structural safety, the deflection δ at the free end of the beam is limited to 5 mm. The deflection of a cantilever beam subjected to a point load P at its free end is given by Eq. (7):

$$\delta = \frac{PL^3}{3EI} \text{..... (7)}$$

By substituting the allowable deflection into Eq. (7), the allowable length of the drone arm is found to be approximately 530 mm**.** This satisfies the deflection limit, indicating that the arm will remain within safe elastic deformation under operational loading.

The maximum bending stress occurs at the fixed end and is computed using Eq. (8):

$$\sigma = \frac{Mc}{I} \text{ ..... (8)}$$

Where M=P·L=21.94Nm and c=h/2=0.02m. Substituting these values, the resulting maximum bending stress is: σ=2.26MPa Since this value is significantly below the tensile strength of ABS (approximately 40 MPa), the design is considered safe against bending failure.

The shear force along the cantilever beam remains constant due to the point load at the free end, as expressed in V(x)=−P=−41.4N and the bending moment at a distance x from the fixed support is described by M(x)=−P(L−x) this moment linearly increases toward the fixed end, with a maximum magnitude of M(0)=−21.94Nm at the fixed support, indicating tension at the top fibers and compression at the bottom.

The transverse shear stress τ is determined using Eq. (9):

$$\tau = \frac{VQ}{It} \text{..... (9)}$$

Here, Q is the first moment of area about the neutral axis, calculated from contributions of the flange and upper half of the web. The flange area is A1=b·t=400mm^2, with centroidal distance y1=15mm. The web area above the neutral axis is A2=t·(h/2−t)=100mm^2, with centroidal distance y2=5mm. The total first moment of area becomes substituting the known values into Eq. (9), the transverse shear stress is:τ=0.1392MPa. This value is significantly lower than the typical shear strength of ABS (20–30 MPa), confirming that the design is safe from shear failure.

The I-beam design offers strong resistance to both bending and shear by concentrating material away from the neutral axis (to resist moment) and using a central web (to resist shear). To refine such structural properties, the parallel axis theorem may be employed, particularly for more complex or composite sections. According to Eq. (10), the total moment of inertia can be expressed as:

$$I_x = I_{xc} + Ad_y^2 \quad ; \quad I_y = I_{yc} + Ad_x^2 \text{.....(10)}$$

This approach allows for adjusting section stiffness based on geometry and mass distribution, making it a powerful tool in generative design systems.

The drone arm is subject to dynamic forces generated by the motor-propeller system, which can induce vibrations. To ensure safe operation, it is critical to evaluate the arm's natural frequency and compare it with the excitation frequency produced during motor rotation.The motor excitation frequency is calculated as:

$$f_m = \frac{\text{RPM}}{60} \text{..... (11)}$$

Using a T-Motor 4008 (KV230) and a 22.2 V battery, the motor speed is: f_m=85.1Hz

The natural frequency of the arm, modeled as a cantilever beam, is given by:

$$f_n = \frac{\beta_1^2}{2\pi}\sqrt{\frac{EI}{\rho AL^4}} \text{ ..... (12)}$$

From Eq. (12) we got f_n=220.589Hz. Since fn≫fm, the arm is safe from resonance [29].

The impact resistance of a hexacopter drone is crucial for ensuring structural integrity during hard landings, especially in agricultural environments. This analysis evaluates the ability of the landing gear particularly the legs to absorb and dissipate the energy from impact without permanent deformation or failure. The kinetic energy at impact is calculated by considering the conversion of potential energy into kinetic energy during free fall:

$$E_{\text{impact}} = mgh \quad \text{..... (13)}$$

Where mmm is the drone mass, g is gravitational acceleration, and h is the landing height. For a drone mass of 16.88 kg and a 10-meter fall, the impact energy is approximately 1655.9 J.

To resist this energy, the landing leg's geometry and material properties play a vital role. The moment of inertia of the leg's rectangular cross-section governs its bending stiffness. While not explicitly needed for this summary, it is used within the stiffness equation and depends heavily on the height and width of the cross-section (height cubed, in particular, greatly influences stiffness). The stiffness of each leg is given by:

$$k_{\text{leg}} = \frac{3EI}{L^3} \quad \text{..... (14)}$$

Where E is Young's modulus, I is the moment of inertia, and L is the leg length. For ABS plastic and a 0.3 m leg, the stiffness per leg is approximately 24.89 kN/m**.** With four legs, the total system stiffness is:

$$K_{\text{total}} = 4 \cdot k_{\text{leg}} = 99.56\,\text{kN/m} \quad \text{..... (15)}$$

The maximum deflection during landing is estimated using energy balance, assuming no energy loss and purely elastic deformation:

$$x = \sqrt{\frac{2E_{\text{impact}}}{K_{\text{total}}}} \quad \text{.....(16)}$$

Substituting the values yields a small deflection of approximately 0.14 mm, indicating high structural rigidity. The impact force transmitted to the structure is:

$$F_{\text{impact}} = K_{\text{total}} \cdot x \quad \text{..... (17)}$$

Resulting in a force of 13.98 kN, which the system must safely absorb. ANSYS simulation (Figure 3) verifies this analytically derived performance. The maximum deformation is 0.00168 m, and the von Mises stress (2.67 MPa) remains well below ABS's yield strength. Furthermore, the elastic strain of 0.00128 confirms full recovery after landing, without permanent damage.

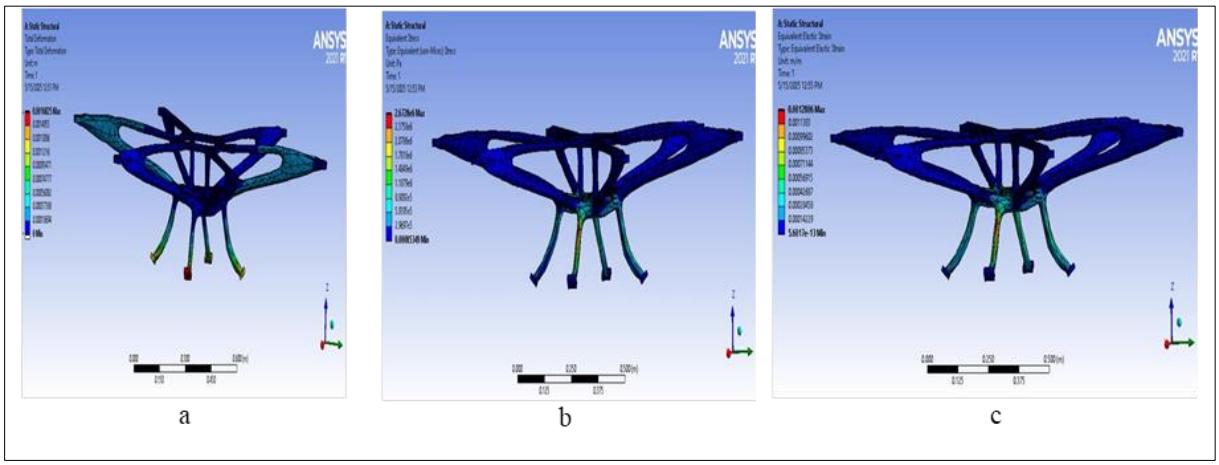

Figure 3 Analysis during landing for a hex copter drone, a) total deformation, b) von mises stress and c) equivalent elastic strain

3.6. Generative Design

In this section, the generative design process is evaluated by simulating real-world operational and boundary constraints relevant to agricultural drone performance. Using Autodesk Fusion 360, preserved regions, obstacle geometries, and applied loads were defined to simulate the structural behavior of the drone frame under flight, landing, and gravitational conditions [9]. These constraints were essential for ensuring that the final design not only met performance requirements but also maintained safety, durability, and functionality during use.

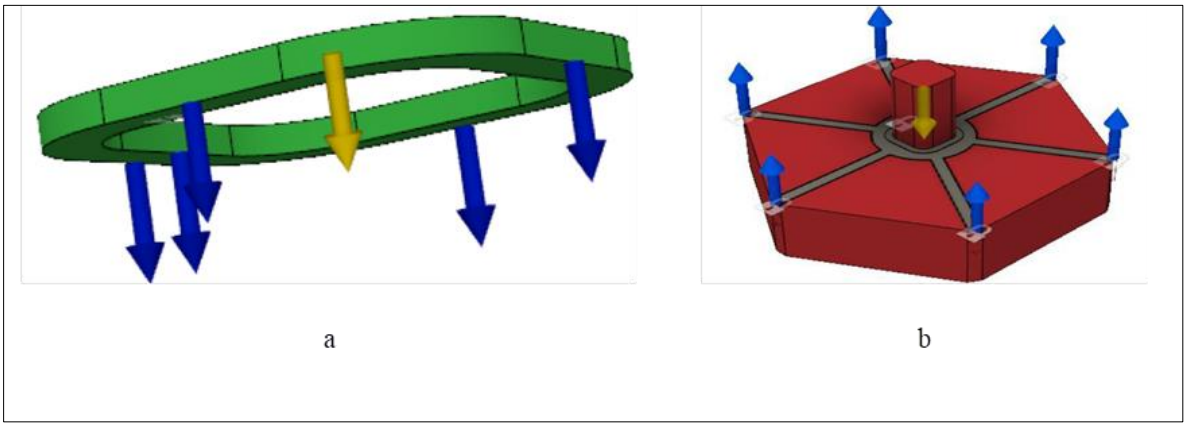

Figure 4 (a) Gravitational force applied at the center of mass. (b) Obstacle geometries (red) and force vectors used in the simulation setup

Further loading conditions are illustrated in Figure 4, where (a) the gravitational force (170 N) is applied vertically downward at the drone's center of mass, simulating its full weight during operation; and (b) red-colored obstacle geometries are defined as material-restricted regions for essential components like the battery compartment, sensor zones, and propeller paths. Blue arrows represent lift forces, while yellow arrows denote gravity direction. These constraints prevent material growth in critical areas and enforce manufacturability and functionality during the optimization phase [9].

Collectively, these loading and constraint conditions guide the AI-driven generative design to produce a structurally optimized drone frame that is lightweight, aerodynamically efficient, and capable of withstanding real-world agricultural deployment stresses.

3.6.1. Generative Design Process and Outcomes

Generative design outcomes for a hexacopter agricultural drone in Autodesk Fusion 360 result from an iterative, algorithm-driven process that explores a wide range of design possibilities. The goal is to optimize objectives such as weight reduction, structural strength, and aerodynamic performance [30]. These outcomes are specifically tailored to meet the forces, constraints, and requirements defined during the simulation setup.

The final drone frame designs typically exhibit organic, lightweight geometries that balance structural rigidity with aerodynamic efficiency. These configurations are optimized to endure lift forces, landing impacts, and vibrational stresses encountered during flight. Many of the solutions incorporate lattice-like patterns or hollow geometries to reduce material while maintaining strength. As a result, the drone design improves safety factors and reduces deflection, making it suitable for UAV applications.

The generative process respects essential constraints including preserved motor mounts, landing leg attachment points, and obstacle zones such as battery bays and sensor mounts. These features ensure that the optimized outputs remain functional, manufacturable, and compatible with other system components. By using this AI-assisted design approach, engineers can generate innovative solutions that are difficult to achieve with traditional CAD methods, ultimately producing efficient and specialized structures for aerial agricultural use.

Figure 5 illustrates two design outcomes created under the same constraint and loading setup in Autodesk Fusion 360. These configurations maintain key functional regions while varying in material distribution and topology.

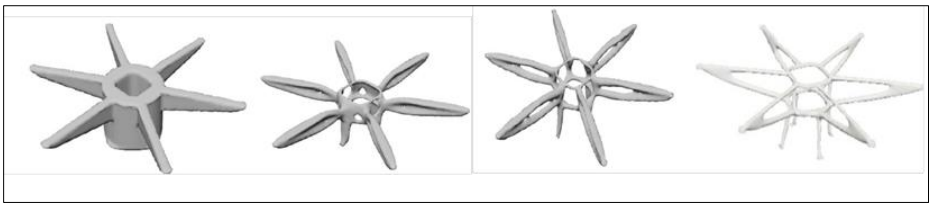

Figure 5 Generative design outcomes in Autodesk Fusion 360 for the drone frame

Key results from the generative design study are visualized in several evaluation plots. As shown in Figure 6, (a) illustrates the relationship between safety factor and global displacement, where an inverse trend is observed—safety factor decreases as displacement increases, highlighting the trade-off between rigidity and flexibility in aerial applications. Similarly, (b) shows how the safety factor increases with mass up to a certain point and then levels off, suggesting that beyond a specific weight, additional mass yields diminishing improvements in structural strength. These insights are essential for optimizing the drone frame's balance between weight, strength, and deformation limits [31].

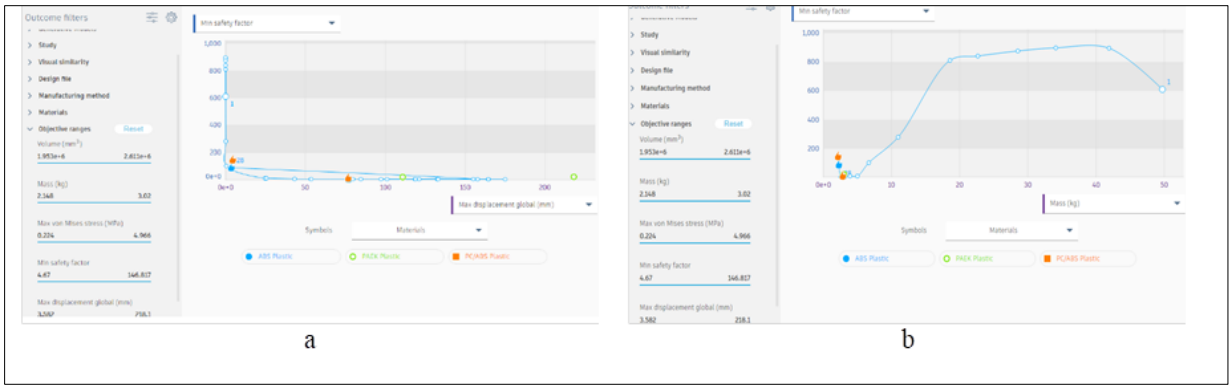

Figure 6 (a) Minimum safety factor vs. maximum global displacement for generative design cases. (b) Minimum safety factor vs. maximum local displacement across evaluated design iterations.

Figure 7 presents two key outputs from the generative design evaluation. (a) illustrates the relationship between maximum von Mises stress and mass for various drone frame designs using different materials (ABS Plastic, PAEK Plastic, PC/ABS Plastic). The plot highlights a trade-off: lighter frames tend to show higher stresses, whereas heavier frames generally exhibit lower stress levels. This analysis helps identify optimal designs that balance strength and weight. (b) provides a tabular summary of recommended design outcomes based on material choice and manufacturing method. Notably, Outcome 2 using ABS plastic and additive manufacturing achieved a 94.055% performance rating, making it the most optimized design for strength, manufacturability, and UAV suitability.

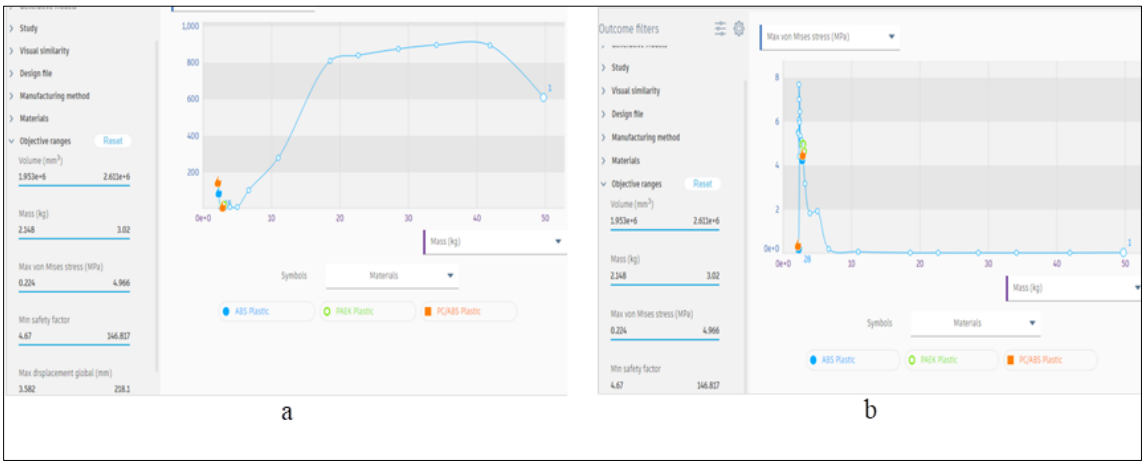

Figure 7 (a) Max von Mises stress (MPa) vs. Mass (kg) for different generative outcomes. (b) Summary of generative design recommendations across materials and methods

Name	Preview Features	Recommendation	Processing status	Generative model	Material	Manufacturing method
Study 1 - Structural ... - Outcome 1		77.61 %	Completed	Generative Model 1	ABS Plastic	Unrestricted
Study 1 - Structural ... - Outcome 2		94.055 %	Completed	Generative Model 1	ABS Plastic	Additive
Study 1 - Structural ... - Outcome 3		0 %	Completed	Generative Model 1	PAEK Plastic	Unrestricted
Study 1 - Structural ... - Outcome 4		0 %	Completed	Generative Model 1	PAEK Plastic	Additive
Study 1 - Structural ... - Outcome 5		56.155 %	Completed	Generative Model 1	PC/ABS Plastic	Unrestricted
Study 1 - Structural ... - Outcome 6		95.748 %	Completed	Generative Model 1	PC/ABS Plastic	Additive

Figure 8 Summary of generative design outcomes with performance metrics

Figure 8 presents a tabular summary of the generative design process outcomes generated in Autodesk Fusion 360. It includes six different design configurations derived from variations in material type—ABS Plastic, PAEK Plastic, and PC/ABS Plastic—and manufacturing methods (either unrestricted or additive). Each row details critical metrics such as volume, mass, maximum von Mises stress, and minimum safety factor. Among these, *Outcome 2,* which utilizes ABS Plastic with additive manufacturing**,** achieved the highest recommendation rating of 94.055%**,** indicating a high level of optimization. This result suggests that Outcome 2 balances weight efficiency, structural strength, and manufacturability better than the other configurations.

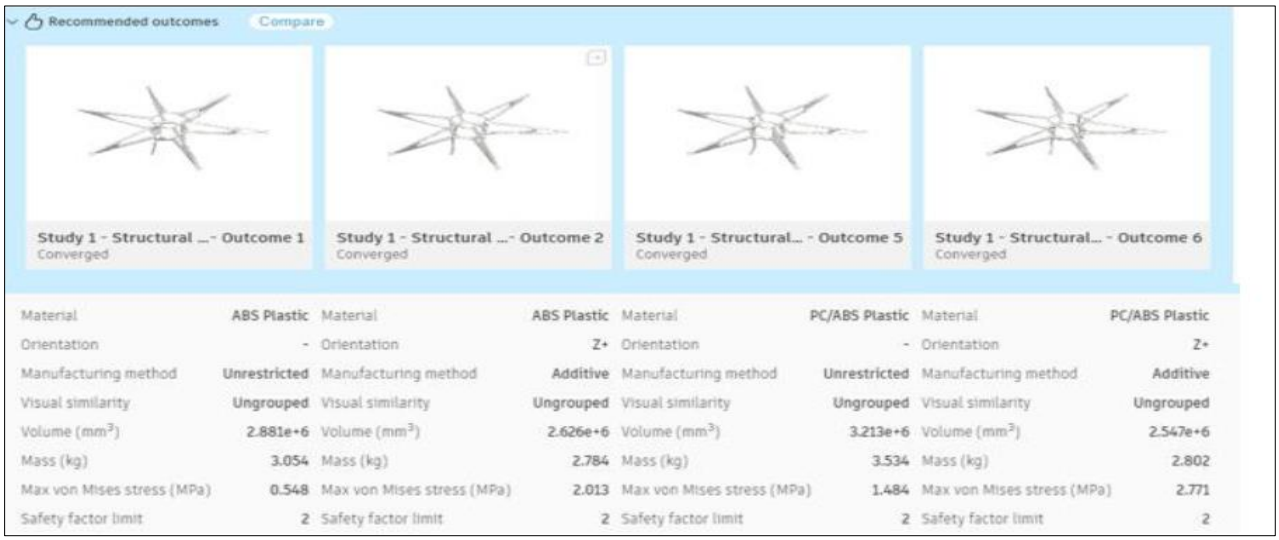

Figure 9 Visual comparison of candidate designs highlighting the optimal solution (Outcome 2) for UAV use

Figure 9 shows a visual comparison of the selected generative design outcomes for the hexacopter frame. It displays four of the six outcomes, illustrating the geometry and volume of each drone frame design. These visual models are aligned with the data shown in Figure 9. Notably, Outcome 2 appears with a compact and organic geometry, optimized to minimize material use while maintaining structural integrity. With a mass of 2.784 kg, a volume of 2.626×10^6 mm^3, a maximum von Mises stress of 2.013 MPa**,** and a safety factor of 2, this design was confirmed as optimal for UAV deployment. The outcome visually reflects key features such as preserved motor zones and a lightweight yet rigid frame topology suitable for additive manufacturing.

3.7. Additive Manufacturing Process and Print Setup

The optimized drone frame was fabricated using Fused Filament Fabrication (FFF) on the MV4BIGM 3D printer, which offers a large print volume and supports nozzle sizes up to 0.8 mm see Table 7 [32]. White ABS filament (1.75 mm) was selected due to its balanced strength and flexibility, with material properties shown in Table 4.

Table 4 Specification of MV4BIGM printer and (b)

Specification	Details
Print Volume	1,010 × 1,010 × 1,010 mm
Machine Dimensions (W × D × H)	1,300 × 1,470 × 1,830 mm
Nozzle Sizes	0.4 mm, 0.6 mm, 0.8 mm
Maximum Hot end Temperature	285°C (upgradeable to 500°C)
Supported Filament Diameter	1.75 mm (user-convertible to 3 mm)
Print Speed	Up to 150 mm/s (depends on nozzle size and layer height)
Layer Resolution	0.1 mm to 0.25 mm

The slicing was done using Cura 5.8.1 with a "brim" adhesion type. Nozzle and bed temperatures were set to 210°C and 85°C, respectively. A tree-support structure and 20% infill were used to ensure print quality and reduce weight. The total print time was 1 day, 21 hours, and 23 minutes. As shown Figure 10 the 3D print preview, illustrating the support regions (red) and drone frame geometry (cyan), confirming proper setup for successful manufacturing.

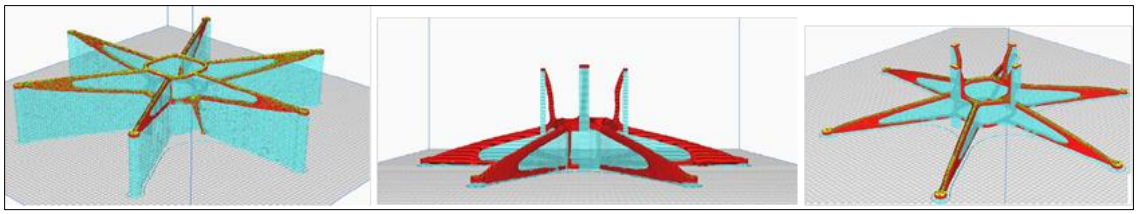

Figure 10 Preview of 3D print on the MV4BIGM printer on Ultimaker Cura 5.8.1

4. Results and Discussion

4.1. Analysis on Generative Design Hexacopter Drone Frame

A detailed structural and mechanical analysis was performed to evaluate the performance, stability, and safety of the generative design drone frame under flight-related operational conditions. Simulations were executed using Fusion 360 with clearly defined boundary conditions, material assignments, and mechanical loads, reflecting realistic flight and landing scenarios. The results discussed here assess whether the frame meets the performance objectives, including high stiffness-to-weight ratio, elastic deformation limits, and robustness under external loading [33].

The generative design was discretized using a fine mesh of 90,749 nodes and 51,999 elements. Parabolic elements, adaptive sizing, and curvature refinement were applied to capture stress concentrations and deformation accurately, especially in thin-walled arms and joints. This ensured realistic FEM simulation and minimized computational errors [34].

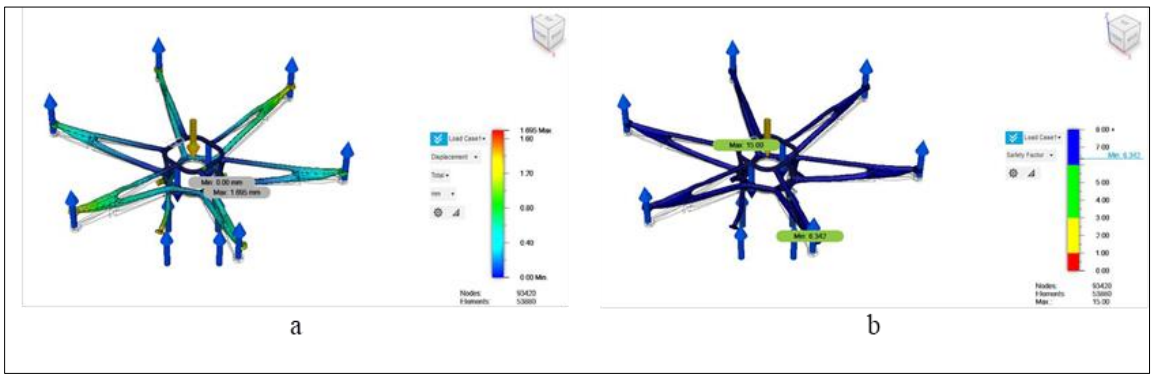

Figure 11 (a) Total deformation analysis of the hexacopter drone frame. (b) Structural safety factor distribution of the hexacopter drone frame

The structural deformation results under upward lift forces and self-weight showed that the maximum total displacement occurred at the outer motor arms due to cantilever effects, with values ranging from 0.00 mm to 1.695 mm, as seen in Figure 11 (a). The upward thrust of 41.4 N from each motor balanced the drone's weight, and the limited deflection confirms sufficient rigidity for stable flight. Additionally, the safety factor distribution, shown in (b), ranged from 6.342 to 15.00, indicating strong mechanical resilience. These values exceed typical safety requirements and suggest that while the central body is slightly over-engineered, the outer arms are efficiently optimized. This balance supports both structural integrity and potential for further weight reduction in future designs [35].

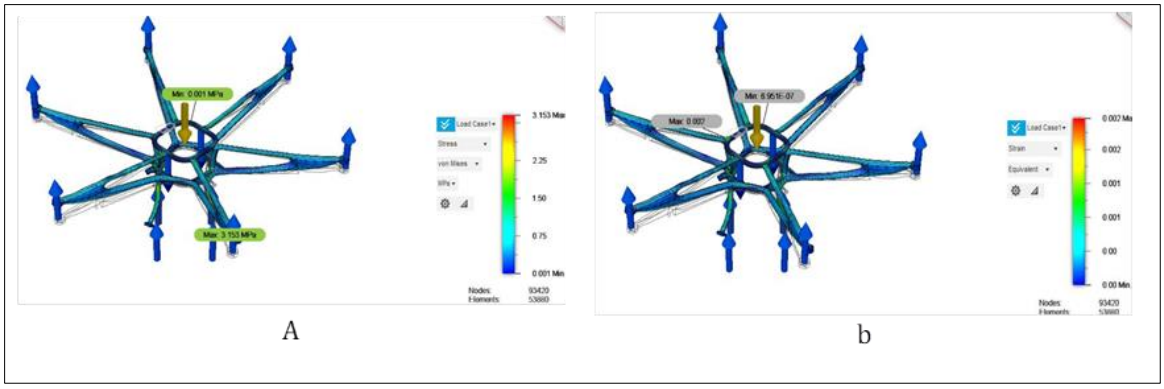

Figure 12 (a) Von Mises stress analysis of the hexacopter drone frame. (b) Equivalent strain distribution of the hexacopter drone frame

The von Mises stress analysis, shown in Figure 12 (a), revealed a maximum stress of 3.153 MPa, which is well below the 43 MPa tensile strength of ABS material. This indicates that no region of the frame is at risk of yielding, with stress concentrated around motor mounts and ribs—areas expected to experience high load transfer. The equivalent strain distribution in (b) showed a maximum of 0.002 mm/mm, confirming elastic behavior throughout the structure. Strain concentrations were mainly observed at the arm joints, yet all values remained safely within the material's elastic range, ensuring that no permanent deformation occurs under normal loading conditions.

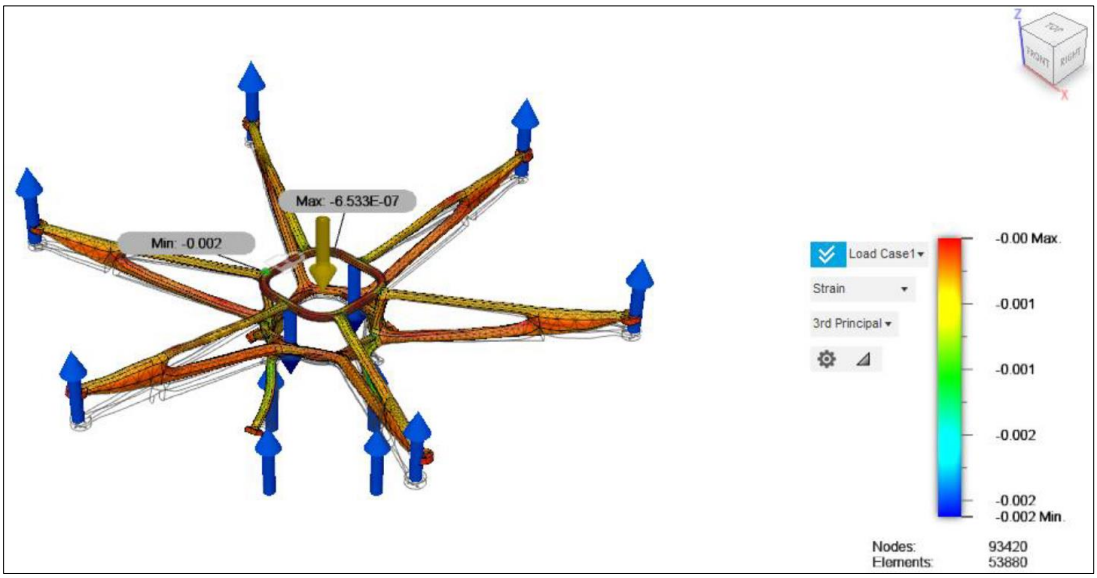

Figure 13 The third principal strain analysis of the hexacopter drone.

Compressive strains, as shown in Figure 13, ranged from –0.002 to 0.00 mm/mm and were primarily concentrated around the inner arms, indicating minimal axial compression. These low values, far below the failure threshold of aerospace-grade ABS, confirm that the structure is safe from buckling or localized crushing. The uniform distribution also reflects well-balanced load paths. Overall, the generative drone frame maintains strength, flexibility, and structural efficiency under normal operational loads, confirming its suitability for lightweight aerial applications.

4.2. Agricultural Drone Flight and Payload Result

The flight performance of the agricultural drone was evaluated under varying liquid payload levels to assess its energy efficiency and endurance. As the drone consumes liquid during operation, its total mass decreases, reducing power requirements and increasing flight time. The relationship between payload weight and flight time is directly influenced by throttle demand and mass. At full tank capacity (10 L), the drone weighs 16.88 kg and requires 80% throttle to maintain hover, limiting flight time to 6 minutes. As the tank empties, the drone becomes lighter, reducing throttle needs: 68.2% at 14.38 kg (three-quarter tank), 56.3% at 11.88 kg (half tank), and 44.45% at 9.38 kg (quarter tank). When the tank is empty (6.88 kg), only 32.6% throttle is needed, achieving a maximum flight time of 14.6 minutes. Table 5 summarizes the detailed values of mass, throttle, and flight time for each payload level.

Table 5 Agricultural drone flight time and Payload Result

No	Lavel of liquid	Total mass of the drone	Throttle	Liter	Flight time
1	Full tank	16.88 kg	80%	10 L	6 min
2	Three-quarter	14.38 kg	68.2%	7.5 L	7 min
3	Half tank	11.88 kg	56.3%	5 L	8.44 min
4	Quarter tank	9.38 kg	44.45%	2.5 L	10.69 min
5	Empty tank	6.88 kg	32.6%	0 L	14.6 min

The performance trends are further illustrated using Figures 14 (a) and (b), which demonstrate the inverse relationships between flight time and throttle percentage, and between flight time and drone mass. These graphs highlight that as the payload decreases, throttle demand drops and flight time increases significantly. The results confirm the design's energy efficiency and operational effectiveness under varying load conditions, emphasizing the benefits of lightweight drone frames for agricultural missions [36].

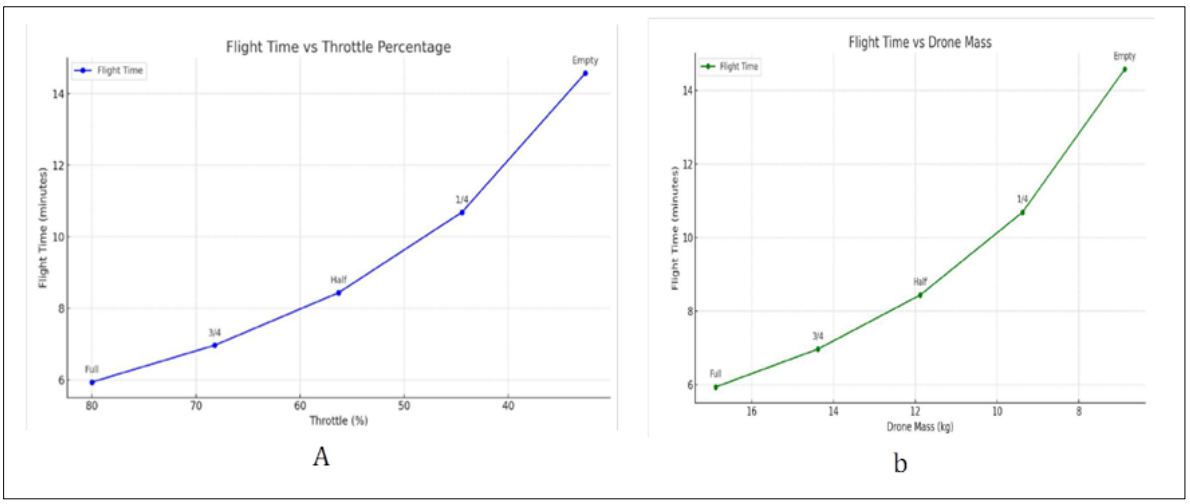

Figure 14 (a) Flight time vs. throttle percentage. (b) Flight time vs. drone total mass

4.3. Validate Agricultural Hexacopter Drone Frame to Real-World Agricultural Drones

The validation process evaluates whether the mass of the generatively designed hexacopter drone frame is practical and competitive for real-world agricultural applications involving a 10-liter payload. The frame mass was compared against industry benchmarks to assess structural efficiency, material use, and weight optimization. As shown in Table 6, the generative drone frame has a mass of 2.784 kg, which is lighter than all listed commercial alternatives. Compared to the DJI Agras T20 frame (3.5 kg), the optimized frame is 20.5% lighter. The weight savings are even more substantial when compared to larger models like the Tarot T18 (4.5 kg), which reflects a 38.1% reduction.

Table 6 Validate agricultural hexacopter drone frame to real-world agricultural drones

No.	Drone Frame Model	Frame Mass (kg)	Material	Hexcopter Frame Mass (kg)	Percentage Difference Mass Optimizing	Reference
1	DJI Agras T20	3.5	Carbon fiber, composites	2.784	-20.5% (lighter)	DJI Agras T20
2	XAG V Series (V40)	4.0	Aluminum alloy, carbon fiber	2.784	-30.4% (lighter)	XAG V Series
3	Hanhe 10L Frame	3.0	Carbon fiber	2.784	-7.2% (lighter)	Hanhe Frames on AliExpress
4	Fly Dragon FD-10	3.2	Carbon fiber, high-strength plastic	2.784	-13.0% (lighter)	Fly Dragon FD-10 on Alibaba
5	Tarot T18 Octocopter	4.5	Aluminum, carbon fiber	2.784	-38.1% (lighter)	Tarot T18 on Banggood

The comparative table demonstrates that despite using lightweight materials such as aluminum and carbon fiber, commercial frames remain heavier than the proposed design. This indicates the effectiveness of generative design in minimizing excess material while preserving structural integrity. The validated frame outperforms competitors like the Hanhe 10L and Fly Dragon FD-10 by 7.2% and 13.0% respectively. These results are graphically depicted in Figure 15, which confirms that the generative design approach achieves significant reductions in structural mass without compromising functionality or durability. This highlights the frame's advantage in payload efficiency and confirms its suitability for aerial spraying applications requiring endurance and load minimization.

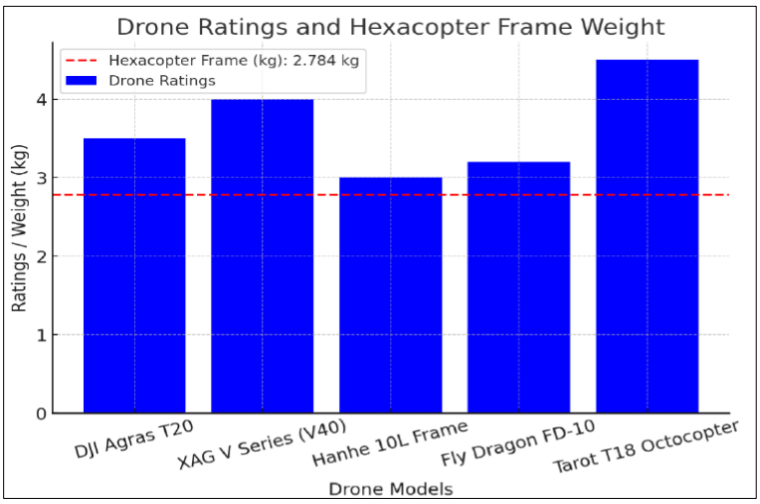

Figure 15 Mass comparison between generative drone frame and commercial agricultural drone frames

5. Conclusion

This research successfully demonstrated the potential of generative design in Autodesk Fusion 360 for developing a structurally efficient and lightweight hexacopter drone frame tailored for agricultural spraying applications. By utilizing topology optimization and setting appropriate design constraints, a final frame mass of 2.784 kg was achieved using ABS plastic via FDM 3D printing. This outcome represents a significant mass reduction of 7.2% to 38.1% compared to existing commercial drone frames designed for 10-liter payload capacity. Structural validation through finite element method (FEM) analysis confirmed that the generative frame design maintained acceptable mechanical integrity under realistic loading conditions. The safety factor ranged from 9.60 to 15, and the maximum deformation was limited to

1.288 mm, ensuring mechanical robustness even under motor thrust and payload-induced stresses. Von Mises stress (3.153 MPa) and strain (0.002 mm/mm) levels remained well within the allowable limits for ABS material, with a compressive third principal strain of only –0.002 mm/mm, indicating full elastic behavior and no risk of buckling.

Flight testing under variable payloads further demonstrated the energy efficiency of the design. As the drone's tank gradually emptied from 10 L to 0 L, total mass decreased from 16.88 kg to 6.88 kg, leading to a reduction in throttle from 80% to 32.6%, and extending flight time from 6.0 to 14.6 minutes. This inverse relationship between payload and flight duration was quantitatively captured using graphs of throttle vs. flight time and drone mass vs. flight time. The drone's efficient hover performance, validated by both simulation and real-world trials, confirms that the lightweight generative design enables superior energy usage and prolonged aerial operation—critical factors for agricultural drones performing coverage-intensive spraying.

In benchmarking studies, the proposed frame was compared to five real-world commercial drones such as the DJI Agras T20, XAG V40, and Tarot T18. The generative design frame was found to be lighter by 7.2% to 38.1%, depending on the competitor, without sacrificing functionality or structural safety. This positions the design as a strong candidate for low-cost, 3D-printed agricultural drones, especially in emerging economies or remote farming areas where affordability, efficiency, and self-manufacturability are key. The research confirms that integrating generative design and additive manufacturing can revolutionize drone development by enabling lightweight, structurally sound, and customized designs suited for field use.

Future work will focus on enhancing drone prototypes with modular payload bays, sensor integration, and AI-based precision spraying. These improvements aim to extend capabilities beyond fluid dispersion by supporting tasks like crop monitoring and adaptive mission planning. Integrating intelligent systems will optimize performance under varying field conditions. This evolution will reinforce the drone's role in smart agriculture

Compliance with ethical standards

Acknowledgments

The authors extend their sincere appreciation to all individuals and institutions who contributed to the successful completion of this study.

Disclosure of conflict of interest

The authors declare no potential conflicts of interest concerning the research, authorship, or publication of this article.

References

[1] M. F. Aslan, A. Durdu, K. Sabanci, E. Ropelewska, and S. S. Gültekin, "A comprehensive survey of the recent studies with UAV for precision agriculture in open fields and greenhouses," Applied Sciences, vol. 12, no. 3, p. 1047, 2022, doi: https://doi.org/10.3390/app12031047.

[2] K. Nonami, F. Kendoul, S. Suzuki, W. Wang, and D. Nakazawa, Autonomous flying robots: unmanned aerial vehicles and micro aerial vehicles. Springer Science and Business Media, 2010.

[3] C. Zhang and J. M. Kovacs, "The application of small unmanned aerial systems for precision agriculture: a review," Precision agriculture, vol. 13, pp. 693-712, 2012, doi: https://doi.org/10.1007/s11119-012-9274-5.

[4] C. H. S. Lee, S. K. Phang, and H. K. Mun, "Design and implementation of an agricultural UAV with optimized spraying mechanism," in MATEC Web of Conferences, 2021, vol. 335: EDP Sciences, p. 02002, doi: https://doi.org/10.1051/matecconf/202133502002.

[5] G. Brunori, "Agriculture and rural areas facing the "twin transition": principles for a sustainable rural digitalisation," Italian Review of Agricultural Economics (REA), vol. 77, no. 3, pp. 3-14, 2022, doi: https://doi.org/10.36253/rea-13983.

[6] K. Telli et al., "A comprehensive review of recent research trends on unmanned aerial vehicles (uavs)," Systems, vol. 11, no. 8, p. 400, 2023, doi: https://doi.org/10.3390/systems11080400.

[7] C. da Silva Junior, M. Pereira, and A. Passaro, "A Systematic Study on Solving Aerospace Problems Using Metaheuristics," arXiv preprint arXiv:2411.02574, 2024.

[8] S. Nvss, B. Esakki, L.-J. Yang, C. Udayagiri, and K. S. Vepa, "Design and development of unibody quadcopter structure using optimization and additive manufacturing techniques," Designs, vol. 6, no. 1, p. 8, 2022, doi: https://doi.org/10.3390/designs6010008.

[9] S. Souvanhnakhoomman and A. Chua, "A COMPREHENSIVE REVIEW OF GENERATIVE DESIGN APPLICATIONS IN UNMANNED AERIAL VEHICLES," ASEAN Engineering Journal, vol. 15, no. 1, pp. 163-175, 2025.

[10] P. Ficzere, "Weight reduction of a drone using generative design," Hungarian Journal of Industry and Chemistry, 2021, doi: DOI: 10.33927/hjic-2021-16.

[11] B. Vayre, F. Vignat, and F. Villeneuve, "Designing for additive manufacturing," Procedia CIrP, vol. 3, pp. 632-637, 2012, doi: https://doi.org/10.1016/j.procir.2012.07.108.

[12] R. O. Ogunleye, S. Rusnáková, J. Javořík, M. Žaludek, and B. Kotlánová, "Advanced Sensors and Sensing Systems for Structural Health Monitoring in Aerospace Composites," Advanced Engineering Materials, vol. 26, no. 22, p. 2401745, 2024, doi: https://doi.org/10.1002/adem.202401745.

[13] V. A. Kumar, M. Sivaguru, B. R. Janaki, K. S. Eswar, P. Kiran, and R. Vijayanandh, "Structural optimization of frame of the multi-rotor unmanned aerial vehicle through computational structural analysis," in Journal of Physics: Conference Series, 2021, vol. 1849, no. 1: IOP Publishing, p. 012004, doi: http://dx.doi.org/10.1088/1742-6596/1849/1/012004.

[14] Z. Liu and K. Karydis, "Dynamic Modeling and Analysis of Impact-resilient MAVs Undergoing High-speed and Large-angle Collisions with the Environment," in 2023 IEEE/RSJ International Conference on Intelligent Robots and Systems (IROS), 2023: IEEE, pp. 4285-4292, doi: https://doi.org/10.1109/IROS55552.2023.10341848.

[15] A. Mishra, S. Pal, G. S. Malhi, and P. Singh, "Structural analysis of UAV airframe by using FEM techniques: A review," International Journal of Advanced Science and Technology, vol. 29, pp. 195-204, 2020.

[16] M. E. Gutierrez-Rivera et al., "Design, Construction and Finite Element Analysis of a Hexacopter for Precision Agriculture Applications," Modelling, vol. 5, no. 3, pp. 1239-1267, 2024, doi: https://doi.org/10.3390/modelling5030064.

[17] A. Nettekoven and U. Topcu, "A 3D printing hexacopter: Design and demonstration," in 2021 International Conference on Unmanned Aircraft Systems (ICUAS), 2021: IEEE, pp. 1472-1477, doi: https://doi.org/10.1109/ICUAS51884.2021.9476759.

[18] D. Lattanzi and G. Miller, "Review of robotic infrastructure inspection systems," Journal of Infrastructure Systems, vol. 23, no. 3, p. 04017004, 2017, doi: https://doi.org/10.1061/(ASCE)IS.1943-555X.0000353.

[19] V. Puri, A. Nayyar, and L. Raja, "Agriculture drones: A modern breakthrough in precision agriculture," Journal of Statistics and Management Systems, vol. 20, no. 4, pp. 507-518, 2017, doi: https://doi.org/10.1080/09720510.2017.1395171.

[20] J. Peksa and D. Mamchur, "A review on the state of the art in copter drones and flight control systems," Sensors, vol. 24, no. 11, p. 3349, 2024, doi: https://doi.org/10.3390/s24113349.

[21] Y. Edan, G. Adamides, and R. Oberti, "Agriculture automation," Springer handbook of automation, pp. 1055-1078, 2023.

[22] B. Rankouhi, S. Javadpour, F. Delfanian, and T. Letcher, "Failure analysis and mechanical characterization of 3D printed ABS with respect to layer thickness and orientation," Journal of Failure Analysis and Prevention, vol. 16, pp. 467-481, 2016.

[23] C. Quental, J. Reis, J. Folgado, J. Monteiro, and M. Sarmento, "Comparison of 3 supraspinatus tendon repair techniques–a 3D computational finite element analysis," Computer Methods in Biomechanics and Biomedical Engineering, vol. 23, no. 16, pp. 1387-1394, 2020, doi: https://doi.org/10.1080/10255842.2020.1805441.

[24] K. Tian, J. Li, J. Zeng, A. Evans, and L. Zhang, "Segmentation of tomato leaf images based on adaptive clustering number of K-means algorithm," Computers and Electronics in Agriculture, vol. 165, p. 104962, 2019, doi: https://doi.org/10.1016/j.compag.2019.104962.

[25] E. Kurt, A. Y. Arabul, F. Keskin Arabul, and I. Senol, "A Multi-Phase Brushless Direct Current Motor Design and Its Implementation in Medium-Altitude Long-Endurance Unmanned Aerial Vehicles," Applied Sciences, vol. 14, no. 24, p. 11550, 2024, doi: https://doi.org/10.3390/app142411550.

[26] Z. Ramos, H. T. Blair, I. De Barbieri, G. Ciappesoni, F. Montossi, and P. R. Kenyon, "Phenotypic responses to selection for ultrafine wool in Uruguayan Yearling Lambs," Agriculture, vol. 11, no. 2, p. 179, 2021, doi: https://doi.org/10.3390/agriculture11020179.

[27] H. X. Pham, H. M. La, D. Feil-Seifer, and M. Deans, "A distributed control framework for a team of unmanned aerial vehicles for dynamic wildfire tracking," in 2017 IEEE/RSJ international conference on intelligent robots and systems (IROS), 2017: IEEE, pp. 6648-6653, doi: https://doi.org/10.1109/IROS.2017.8206579.

[28] A. Demirtaş and M. Bayraktar, "Free vibration analysis of an aircraft wing by considering as a cantilever beam," Selçuk Üniversitesi Mühendislik, Bilim Ve Teknoloji Dergisi, vol. 7, no. 1, pp. 12-21, 2019, doi: https://doi.org/10.15317/Scitech.2019.178.

[29] S. Eken, "Free vibration analysis of composite aircraft wings modeled as thin-walled beams with NACA airfoil sections," Thin-Walled Structures, vol. 139, pp. 362-371, 2019, doi: https://doi.org/10.1016/j.tws.2019.01.042.

[30] P. Yadav, V. Yadav, V. Francis, and N. Kumar, "Use of a Generative Design Approach for UAV Frame Structure Optimization and Additive Manufacturing," in Advances in Modelling and Optimization of Manufacturing and Industrial Systems: Select Proceedings of CIMS 2021: Springer, 2023, pp. 197-207.

[31] A. Balayan, R. Mallick, S. Dwivedi, S. Saxena, B. Haorongbam, and A. Sharma, "Optimal Design of Quadcopter Chassis Using Generative Design and Lightweight Materials to Advance Precision Agriculture," Machines, vol. 12, no. 3, p. 187, 2024, doi: https://doi.org/10.3390/machines12030187.

[32] T. D. Ngo, A. Kashani, G. Imbalzano, K. T. Nguyen, and D. Hui, "Additive manufacturing (3D printing): A review of materials, methods, applications and challenges," Composites Part B: Engineering, vol. 143, pp. 172-196, 2018, doi: https://doi.org/10.1016/j.compositesb.2018.02.012.

[33] V. Gunasekaran, J. Pitchaimani, and L. B. M. Chinnapandi, "Free vibration and inherent material damping characteristics of boron-FRP plate: influence of non-uniform uniaxial edge loads," International Journal for Simulation and Multidisciplinary Design Optimization, vol. 12, p. 18, 2021, doi: https://doi.org/10.1051/smdo/2021017.

[34] A. M. Rayed, B. Esakki, A. Ponnambalam, S. C. Banik, and K. Aly, "Optimization of UAV structure and evaluation of vibrational and fatigue characteristics through simulation studies," International Journal for Simulation and Multidisciplinary Design Optimization, vol. 12, p. 17, 2021, doi: https://doi.org/10.1051/smdo/2021020.

[35] B. Bay and M. Eryıldız, "Design and Analysis of a Topology-Optimized Quadcopter Drone Frame," Gazi University Journal of Science Part C: Design and Technology, vol. 12, no. 2, pp. 427-437, 2024, doi: https://doi.org/10.29109/gujsc.1316791.

[36] J. Li et al., "Rapid evaluation model of endurance performance and its application for agricultural UAVs," Drones, vol. 6, no. 8, p. 186, 2022, doi: https://doi.org/10.3390/drones6080186.